A Multi-Dwell Temperature Profile Design for the Cure of Thick CFRP Composite Laminates

Wenchang Zhang
Northwestern Polytechnical University
Yingjie Xu (xu.yingjie@nwpu.edu.cn)
Engineering Simulation and Aerospace Computing (ESAC)
Xinyu Hui
Northwestern Polytechnical University
Weihong Zhang
Northwestern Polytechnical University

Research Article

Keywords: CFRP, Cure process, Multi-objective optimization, Genetic algorithm, Finite element method

Posted Date: May 18th, 2021

DOI: https://doi.org/10.21203/rs.3.rs-401234/v1

Version of Record: A version of this preprint was published at The International Journal of Advanced Manufacturing Technology on August 5th, 2021. See the published version at https://doi.org/10.1007/s00170-021-07765-1.

A multi-dwell temperature profile design for the cure of thick CFRP composite laminates

Wenchang Zhang[a], Yingjie Xu[a,b,*], Xinyu Hui[a], Weihong Zhang[a]

[a]*State IJR Center of Aerospace Design and Additive Manufacturing, Northwestern Polytechnical University, Xi'an, Shaanxi 710072, China*

[b]*Shaanxi Engineering Laboratory of Aerospace Structure Design and Application, Northwestern Polytechnical University, Xi'an, Shaanxi 710072, China*

Abstract

This paper develops a multi-objective optimization method for the cure of thick composite laminates. The purpose is to minimize the cure time and maximum temperature overshoot in the cure process by designing the cure temperature profile. This method combines the finite element based thermo-chemical coupled cure simulation with the non-dominated sorting genetic algorithm-II (NSGA-II). In order to investigate the influence of the number of dwells on the optimization result, four-dwell and two-dwell temperature profiles are selected for the design variables. The optimization method obtains successfully the Pareto optimal front of the multi-objective problem in thick and ultra-thick laminates. The result shows that the cure time and maximum temperature overshoot are both reduced significantly. The optimization result further illustrates that the four-dwell cure profile is more effective than the two-dwell, especially for the ultra-thick laminates. Through the optimization of the four-dwell profile, the cure time is reduced by 51.0% (thick case) and 30.3% (ultra-thick case) and the maximum temperature overshoot is reduced by 66.9% (thick case) and 73.1% (ultra-thick case) compared with the recommended cure profile. In addition, Self-organizing map (SOM) is employed to visualize the relationships between the design variables with respect to the optimization result.

Keywords: CFRP, Cure process, Multi-objective optimization, Genetic algorithm, Finite element method

*Corresponding author.

Email address: xu.yingjie@nwpu.edu.cn (Yingjie Xu)

1. Introduction

With the increasing demand for high performance and weight reduction in various fields such as aerospace, navigation and automotive, etc., carbon fiber reinforced polymer (CFRP) composites have been widely used due to their high specific stiffness and strength. The large-size composite parts, particularly the primary load-bearing structures in aircraft, are generally manufactured by autoclave cure process [1]. Cure process is one of the most important stage determining the final quality of the composite parts. In a cure process, the temperature and pressure boundaries prescribed in the cure profile are imposed to the prepregs [2]. The cure temperature profile is usually recommended by the prepreg manufacturer, which could provide a guidance for the cure of composite parts. However, the recommended profile is not suitable for all types parts. For instance in the cure of the thick composite parts, the reaction heat cannot be transferred to the surface in time due to the low thermal conductivity of prepreg and the large thickness. The severe temperature overshoots would be generated inside the thick composite parts using the recommended profile and lead to resin degradation, non-uniform cure and residual stress [3] of the parts. In industry, the risks associated with temperature overshoots in thick composite parts are dealt with by adopting conservative cure cycles or trial and error method. This lead to long processing times and high manufacturing costs.

Therefore, it is desirable to achieve an optimal cure temperature profile that can minimize the temperature overshoots or other process-induced defects. The optimization of temperature profile should be based on a comprehensive understanding of the physical state of composite parts during cure. Several experimental works [4–6] have been conducted to monitor the state evolution in a cure process by using temperature, pressure and viscosity sensors. However, experimental approach is complicated and costly, and sensors embed in composite part would perturb the cure process [7]. An effective and relatively inexpensive approach is numerical simulation of the cure process. Numerical models of cure process of thermoset polymer composites have been improved from simple one-dimensional finite difference models [8] to advanced three-dimensional finite element models [9]. Compared with the experimental method [10], simulation models could provide comprehensive information during cure in an efficient way, such as the evolutions of the

temperature, degree of cure, residual stress of cured part and so on [11, 12].

Based on the mature numerical models describing the cure process, determination of optimal cure temperature profiles that can minimize cure time and the occurrence of temperature overshoots or other process-induced defects have been addressed in the literature. Lee applied a sequential unconstrained minimization technique (SUM technique) to design an optimal temperature profile with the cooling and reheating steps to minimize the temperature overshoot [13]. Li et al. combined finite element simulation and a gradient-based optimization tool to minimize the cure time [14]. Ruzi developed a multi-criteria optimization algorithm to minimize the cure residual stresses and maximize the final degree of cure [15]. Kennedy combined a semi-analytic gradient evaluation technique with a gradient-based optimization algorithm to find an optimal cure temperature history to maximize the failure load of the specific structure [16]. Vafayan used genetic algorithm and finite element method to minimize a complete objective weighted by temperature difference and cure difference [17]. Wang proposed an optimization method which decomposed the original problem into several sub-problems to reduce the spring-back during the autoclave cure [18]. Aleksendric et al. integrated the artificial neural networks (ANN) and a fuzzy logic algorithm to adjust the cure profile to obtain a desired trend of degree of cure [19]. Struzziero combined the finite element method with a multi-objective genetic algorithm to minimize the cure time and maximum temperature overshoot [20]. Shah used the multi-objective genetic algorithm to optimize the cure temperature profile to minimize residual stresses and the total cure time of asymmetric laminates cured by autoclave [21]. Dolkun obtained a Pareto front of cure profile in multi-dimensional objective space and cure time, degree of cure difference and temperature difference were minimized simultaneously [22].

In the case of thick composite parts, a two-dwell cure temperature profile is usually considered. For the ultra-thick parts, it is expected that increasing the dwell could achieve improvement in temperature overshoot compared to standard cure profiles. Sorrentino defined a preliminary methodology which inserting an additional dwell placed between the two original dwell to avoid resin degradation and decrease the temperature overshoot [23, 24]. The duration of the additional dwell is heuristically determined and needs further study to be optimal. Jahromi used a trained dynamic ANN instead of finite element calculation and the non-linear programming algorithm to

design multi-dwell temperature profile with the objective to minimize the maximum temperature difference during the curing [25]. However, the study only considered the improvement of cure quality and the cure time was pre-defined.

This paper is devoted to develop a multi-dwell temperature profile design methodology for thick CFRP composite laminates. Compared with the existed studies, the influence of the number of dwells on the optimization results is investigated. The two objectives, i.e. the cure time and maximum temperature overshoot in the cure process are minimized simultaneously using a multi-objective Genetic Algorithm (GA). A thermo-chemical coupled simulation model of the cure process is combined with the GA. The proposed methodology is applied to the cure of a thick AS4/8552 laminate. The optimization result shows the cure time and temperature overshoot are effectively decreased by the multi-dwell temperature profile design.

2. Thermo-chemical coupled model of the cure process

2.1. Theoretical formulation

During the cure process, the composites are subjected to external temperature profile. The cure reaction of resin depends on the temperature. Meantime, the cure reaction of the resin releases the heat. Therefore, the heat transfer process and the cure reaction process couple with each other. To solve this problem, a thermo-chemical coupled simulation incorporating the heat transfer model and cure kinetics model is considered in this study. The thermo-chemical coupled heat transfer equation is expressed as [26]:

$$\rho C_p \frac{\partial T}{\partial t} = K_{xx}\frac{\partial^2 T}{\partial x^2} + K_{yy}\frac{\partial^2 T}{\partial y^2} + K_{zz}\frac{\partial^2 T}{\partial z^2} + \dot{q} \tag{1}$$

where ρ and C_p are the density and specific heat capacity of the composites, respectively, T is the current temperature, $K_{ii}(i = x, y, z)$ is the conductivity of the composites in different directions, $\dot{q}$ is the internal heat released in the cure reaction, which can be quantitatively expressed as:

$$\dot{q} = \rho_r V_r H_r \frac{d\alpha}{dt} \tag{2}$$

where ρ_r is the density of the resin, V_r is the volume fraction of the resin, H_r is the heat generated by the complete reaction of unit mass of resin. $\frac{d\alpha}{dt}$ is the instantaneous cure rate of the resin and can be determined by the cure kinetics model and material type. In this study, the AS4/8552 prepregs are adopted and the cure kinetic model used in [27] is employed as:

$$\frac{d\alpha}{dt} = \frac{k\alpha^m(1-\alpha)^n}{1+e^{C_\alpha(\alpha-\alpha_C)}} \tag{3}$$

where α is the degree of the cure. m and n are reaction orders obtained by fitting the result of DSC experiment. k is reaction rate constants expressed as follows:

$$k = Ae^{(-\Delta E/RT)} \tag{4}$$

where A is pre-exponential factor, E is the activation energy for the chemical reaction, T is the absolute temperature, R is the universal gas constant and C_α is the diffusion constant, which can be calculated by:

$$\alpha_C = \alpha_{C0} + \alpha_{CT}T \tag{5}$$

where α_{C0} is the constant at the temperature is absolute zero, and α_{CT} is the slope in the linear relationship between temperature and α_C. parameter values of the cure kinetics model from [27] are used in this study and listed in Table 1.

Table 1: Cure kinetics model of 8552 epoxy resin.

Parameters	Value
A [s^{-1}]	70000
E [J]	65000
m	0.5
n	1.5
C_α	30
α_{C0}	−1.515
α_{CT} [K^{-1}]	5.171E−3
H_r [J/K]	574000

The properties of composites are evaluated with the rule of mixture. The specific heat capacity

of the composites C_p is calculated as [28, 29]:

$$C_p = V_f C_f + (1 - V_f) C_r \tag{6}$$

where V_f is the volume fraction of the fiber. C_r and C_f are the specific heat of the resin and fiber, respectively.

Similarly, the thermal conductivity of composites in longitudinal direction K_{xx} and transverse direction K_{yy} and K_{zz} are computed as follows:

$$K_{xx} = V_f K_{lf} + (1 - v_f) K_r \tag{7}$$

$$K_{yy} = K_{zz} = K_r \left\{ (1 - 2\sqrt{V_f/\pi}) + \frac{1}{B} \left[\pi - \frac{4}{\sqrt{1 - B^2 V_f/\pi}} \tan^{-1} \frac{\sqrt{1 - B^2 V_f/\pi}}{1 + B\sqrt{V_f/\pi}} \right] \right\} \tag{8}$$

where $B = 2(\frac{K_r}{K_{tf}} - 1)$, K_{lf} and K_{tf} are the thermal conductivities of the fiber in longitudinal direction and transverse direction, K_r is the thermal conductivity of the 8552 epoxy resin. The values in the material models are listed in Table 2. The thermal properties of AS4 fiber and 8552 epoxy resin from [28, 29] are listed in Table 2.

Table 2: Thermal properties of AS4 fiber and 8552 epoxy resin.

Parameters	Value
K_r [W/(m·K)]	$0.148 + 3.43\text{E} - 3T$
K_{lf} [W/(m·K)]	$2.4 + 5.07\text{E} - 3T$
K_{tf} [W/(m·K)]	$7.69 + 1.56\text{E}{-2}T$
C_r [J/(kg·K)]	$931 + 3.47T$
C_f [J/(kg·K)]	$750 + 2.05T$
ρ	$1790V_f + 1300(1 - V_f)$
V_f	0.574

2.2. *Numerical validation*

In this study, ABAQUS is used to solve the thermo-chemical coupled heat transfer model. The cure kinetics model of the resin, specific heat capacity and thermal conductivities of the composites is all implemented through the user subroutines UMATHT and USEFLD. To verify the accuracy of the thermo-chemical coupled simulation model, a cure simulation of a composite plate sample

from literature [30] are conducted and compared with the reported result. The example is illustrated in Fig 1. Due to the symmetry, only one half of model is developed and a symmetrical insulation boundary condition is applied on the symmetry edge. Two-dimensional 4-node linear heat transfer quadrilateral (DC2D4) elements of ABAQUS are used. The temperature boundary conditions of the model is illustrated in Fig 1. The temperature profile illustrated in Fig 2 is imposed on the sample bottom surface contacted with the tool. The first and second heating rates are both 2 °C/min. The first dwell is 110 °C for 60 min and the second dwell is 180 °C for 170 min. The heating air continuously flows across the surface of composite sample for heat exchange and a convective boundary condition is applied on the sample surface.

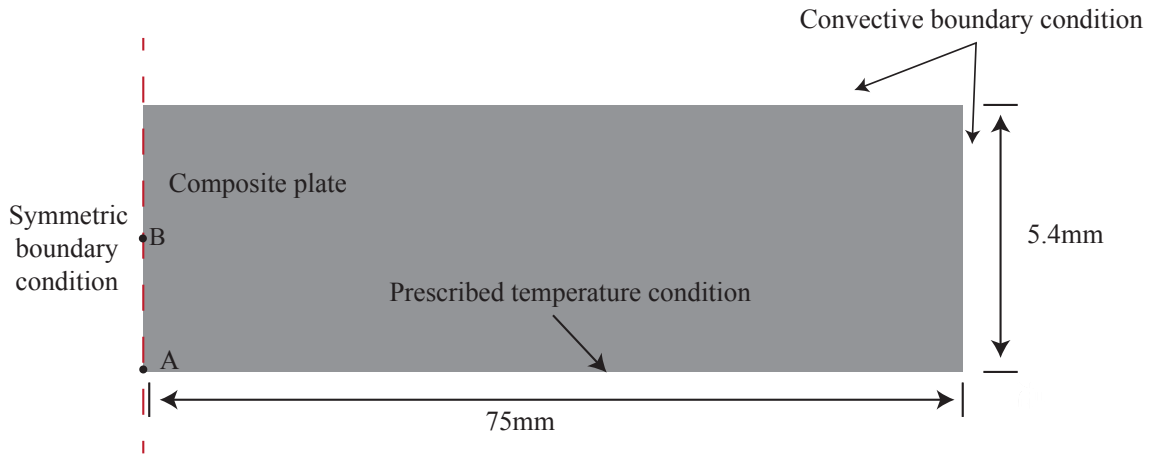

Figure 1: Schematic of the validated model.

The simulation results are shown in Fig 3. The histories of the temperature and the degree of cure at point A and point B are compared with the literature data. As can be seen, the simulation result coincides well with the literature data.

3. Multi-objective optimization

3.1. Problem description

Two cases of AS4/8552 unidirectional laminates, i.e. the 24 mm thick laminate and the 50 mm ultra-thick laminate are considered respectively. 24 mm and 50 mm are the typical dimensions of thick and ultra-thick composite parts which are common accepted in aerospace engineering [20]. The standard two-dwell temperature profile illustrated in Fig 2 is used to simulate the cure

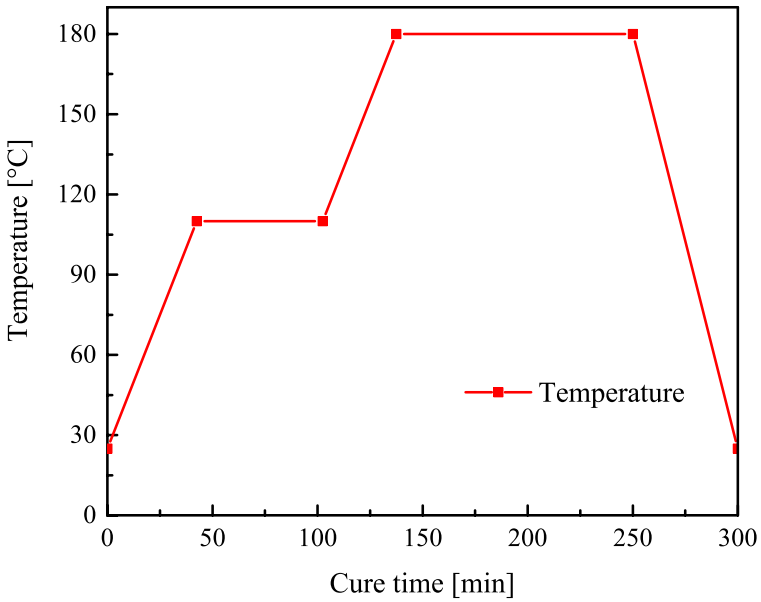

Figure 2: Curing temperature profile used for model validation.

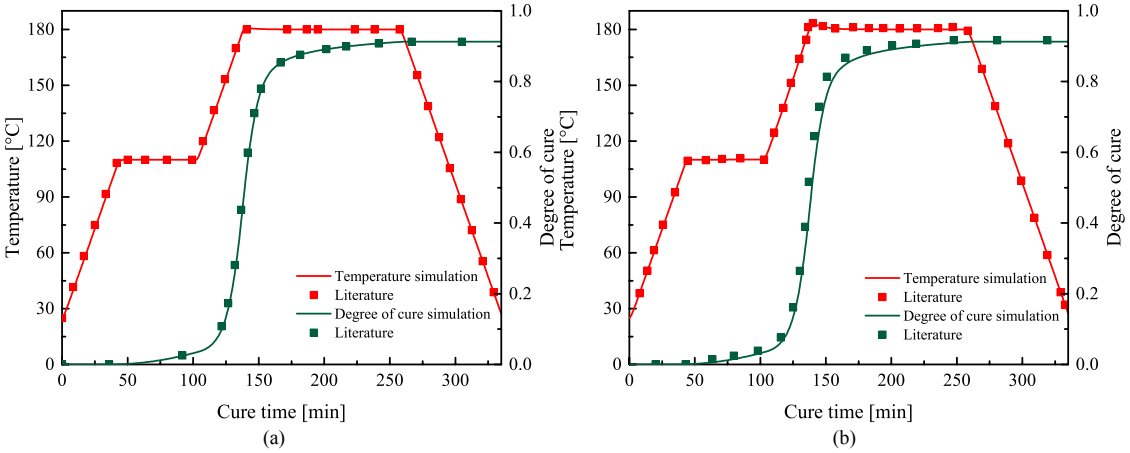

Figure 3: Comparison of simulation result and literature data: (a) Point A, (b) Point B.

process of the two laminates by using the thermo-chemical coupled simulation model. Due to the cure reaction is implemented in the heating and temperature holding stages, the cooling stage is not considered in the simulation [24, 25]. Two 3D finite element models are established. The geometric size of the thick case is 60×60×24 mm^3 and the ultra-thick case is 100×100×50 mm^3. Three-dimensional 8-node linear heat transfer brick (DC3D8) elements of ABAQUS are used.

In the simulation, the surfaces of laminate contacting with the vacuum bag are subjected to air convection and the air temperature is predefined by the cure profile. The convective heat transfer coefficient between the air and the laminate ranges from 30 to 100 W/m^2 [31, 32] and a value 50 W/m^2 is used in this study. The bottom surface of laminate contacting with the tool is imposed to the ambient temperature.

Fig 4 presents the simulation results of the temperature and degree of cure history of the center and bottom of the two laminates. Severe temperature overshoots are observed in the curing process of both two laminates. The maximum temperature difference between the center and bottom reaches 46.5 °C for the thick laminate. For the ultra-thick laminate, the temperature overshoot becomes more serious and the maximum temperature difference reaches 94.63 °C. The simulation results have clearly shown that large temperature overshoot is induced in the thick composite laminates. Moreover, the increase of the thickness of laminates would aggravate the overshoot dramatically. Therefore, it is desirable to develop an optimization method to reduce the gradients of the temperature for composite parts with large thickness.

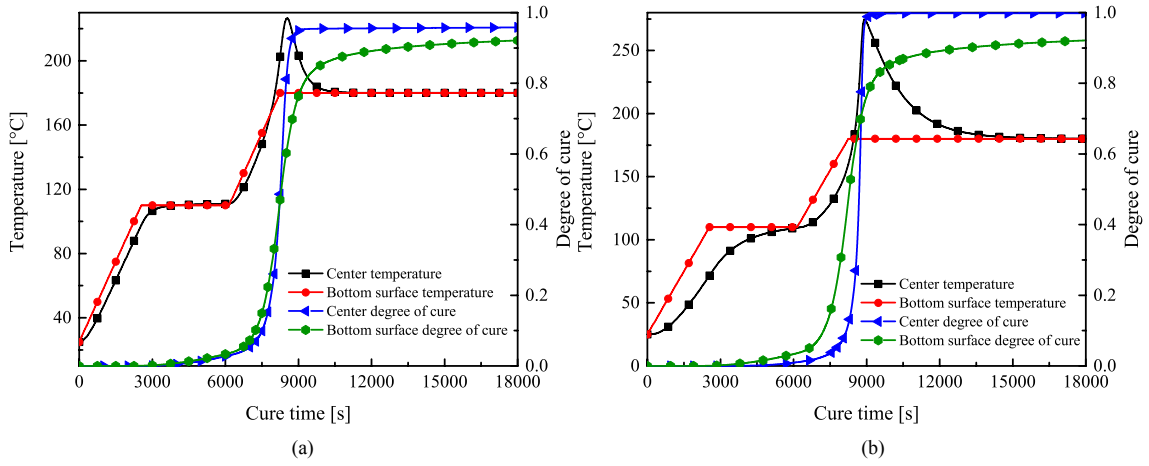

Figure 4: Simulation result of recommended cure profile for (a) thick laminate and (b) ultra-thick laminate.

3.2. Optimization method

Multi-objective optimization is regarded as an effective method that can effectively find the trade-off of the conflict objectives. In this study, the aim of the multi-objective optimization is to minimize the cure time and temperature overshoot through optimizing the cure temperature profile. In order to study the effect of the number of dwell on the optimization result, a four-dwell temperature profile and a two-dwell temperature profile are both considered in the optimizations for the two laminates. The general form of the temperature profiles is illustrated in Fig 5. The four-dwell profile is parameterized using 12 parameters: the heating rate (a_1, a_2, a_3, a_4), the duration of dwell (t_1, t_2, t_3, t_4), the temperature difference between the first dwell and initial temperature (ΔT_1) and the temperature difference between two adjacent dwells (ΔT_2, ΔT_3, ΔT_4). The two-dwell profile is parameterized using 6 parameters: the heating rate (a_1, a_2), the duration of dwell (t_1, t_2), the temperature difference between the first dwell and initial temperature (ΔT_2) and the temperature difference between two adjacent dwells (ΔT_1). These parameters serve as design variables. The ranges of the design variables and the minimum increment for each parameter are listed in Table 3 and Table 4. Considering the reliability of the process control of autoclave, the design variables are needed to be iterated discretely with a minimum increment. In this study the minimum temperature difference of adjacent dwells is set to be 0.1, which means that the adjacent dwells can be fused into one dwell. Considering that a very small temperature fluctuation between two adjacent dwells is impossible to be realized in an actual autoclave process, the adjacent dwells would be fused into one dwell when the optimized result is less than 5 °C.

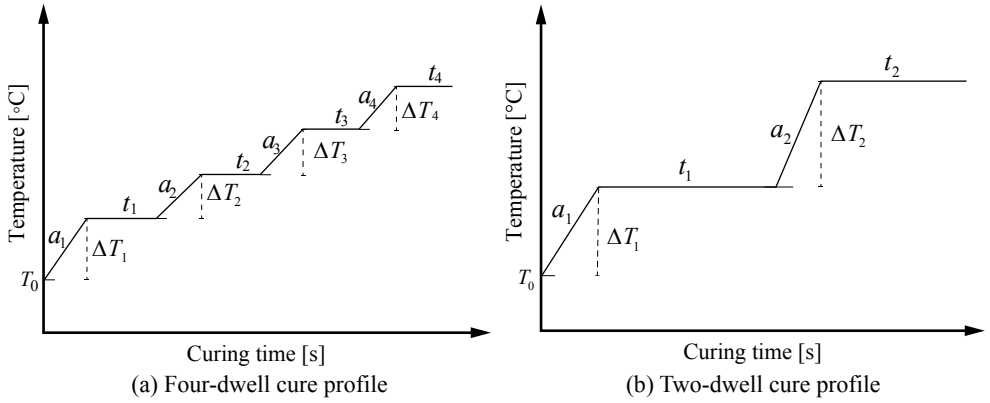

(a) Four-dwell cure profile (b) Two-dwell cure profile

Figure 5: Temperature profiles to be optimized: (a) Four-dwell profile, (b) Two-dwell profile.

Table 3: Range of design variables in four dwell profile.

Parameters	Variation range	Minimum Increment
a_1, a_2, a_3, a_4 [°C/min]	0.5-5.0	0.1
t_1, t_2, t_3, t_4 [s]	60-4500	60
ΔT_1 [°C]	60-120	0.1
ΔT_2, ΔT_3, ΔT_4 [°C]	0-60	0.1

Table 4: Range of design variables in two dwell profile.

Parameters	Variation range	Minimum Increment
a_1, a_2, a_3, a_4 [°C/min]	0.5-5.0	0.1
t_1, t_2, t_3, t_4 [s]	1200-9000	60
ΔT_1 [°C]	60-120	0.1
ΔT_2, ΔT_3, ΔT_4 [°C]	0-120	0.1

It should be noted that the minimum degree of cure at the end of cure process (denoted by α_{min}) is constrained to 0.9, which is a necessary constraint during optimization to ensure that composite part is fully cured. The optimization problem is formulated as:

$$\begin{aligned} Find \quad & X = (a_i, \Delta T_i, t_i) \\ Min \quad & t_{cure},\ \Delta T_{max} \\ S.T. \quad & \alpha_{min} \geq 0.9 \end{aligned} \tag{9}$$

where a_i, ΔT_i, t_i are design variables describing the cure profile, t_{cure} is the cure time, ΔT_{max} is the maximum temperature difference during the cure process.

Considering the discrete nature of the design variables, non-dominated sorting genetic algorithm (NSGA-II) [33] is adopted to solve the optimization problem in this study. The efficiency and reliability of the algorithm were tested with 9 classical calculation examples and the results proved that NSGA-II is able to approximate the Pareto-optimal front quickly [34]. The NSGA-II algorithm is combined with the finite element simulation to implement the multi-objective optimization.

The flowchart of optimization is illustrated in Fig 6. An interface linking the NSGA-II with the ABAQUS Solver is implemented in python. Firstly, the variables population is generated in a random way to create a new cure profile. Secondly, the interface reads the parameter values of the

cure profile and updates the temperature boundary condition in the script file. The script file is then implemented to execute the thermal-chemical coupled simulation in ABAQUS. The temperature and the degree of cure during the cure process are calculated and stored for post-processing. The results of maximum temperature difference ΔT_{max}, cure time t_{total}, and minimum degree of cure α_{min} are extracted into a text file. The interface reads the results and sends them to the NSGA-II to generate a new group of variables. The algorithm parameters are listed in Table 5. The number of generation is 80 and each generation contains 100 independent variable populations. A total 8000 cure profiles are generated for cure simulation during the optimization process to obtain the optimal Pareto front, which takes about 20 hours for a computer with a quad-core processer (2.8 GHz) and 50 GB memory.

Table 5: Parameters of NSGA-II

Parameters	Value
Number of generations	80
Number of individual in the population	100
Crossover distribution index	15
Mutation distribution index	15

4. Optimization results and discussion

The solutions obtained from multi-objective optimization are a series of non-inferior Pareto front, which includes all the optimal solutions presented in objective space. Fig 7 shows the optimal Pareto fronts for the thick and ultra-thick laminates subjected to the four-dwell profile. X and Y axes represent the two objectives, respectively. As shown in Fig 7, the Pareto fronts can be divided into three regions: (1) a vertical region in which cure time can be reduced significantly with large temperature overshoot; (2) a horizon region in which temperature overshoots are reduced significantly with long cure time; and (3) a corner region which achieves a good balance between the cure time and temperature overshoot. The temperature overshoots are reduced with relatively low time consuming.

Moreover, the Pareto fronts from four-dwell and two-dwell profile optimization as well as the result from original recommended profile for the thick and ultra-thick laminates are presented in

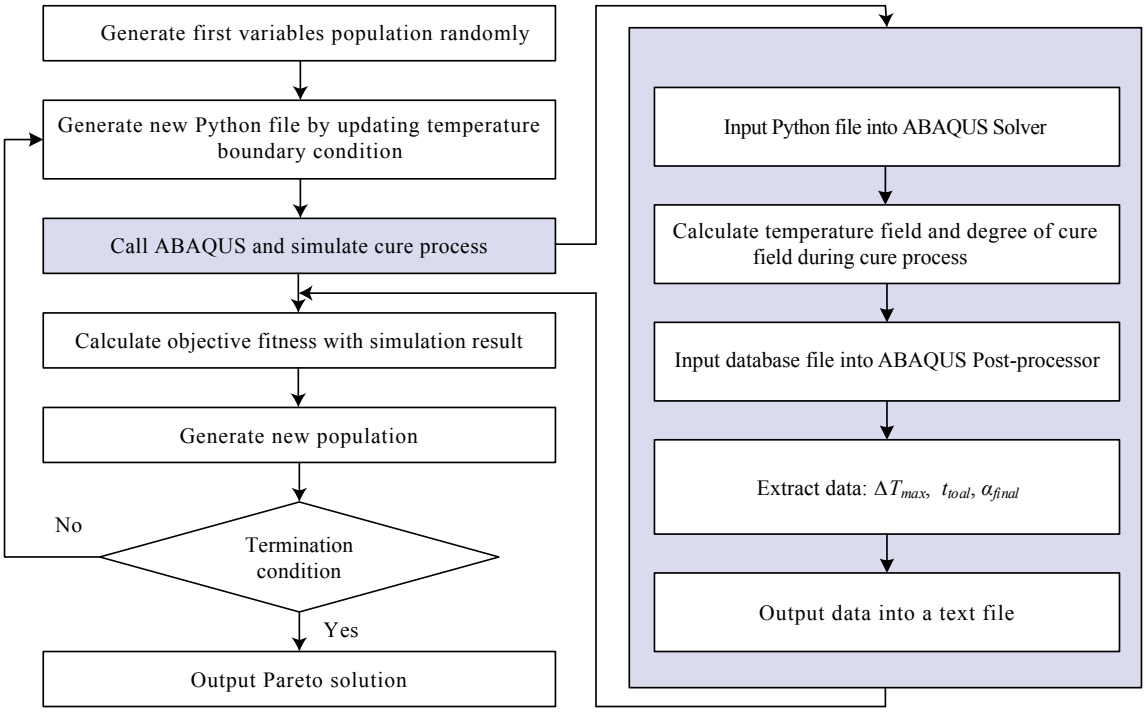

Figure 6: The flowchart of optimization.

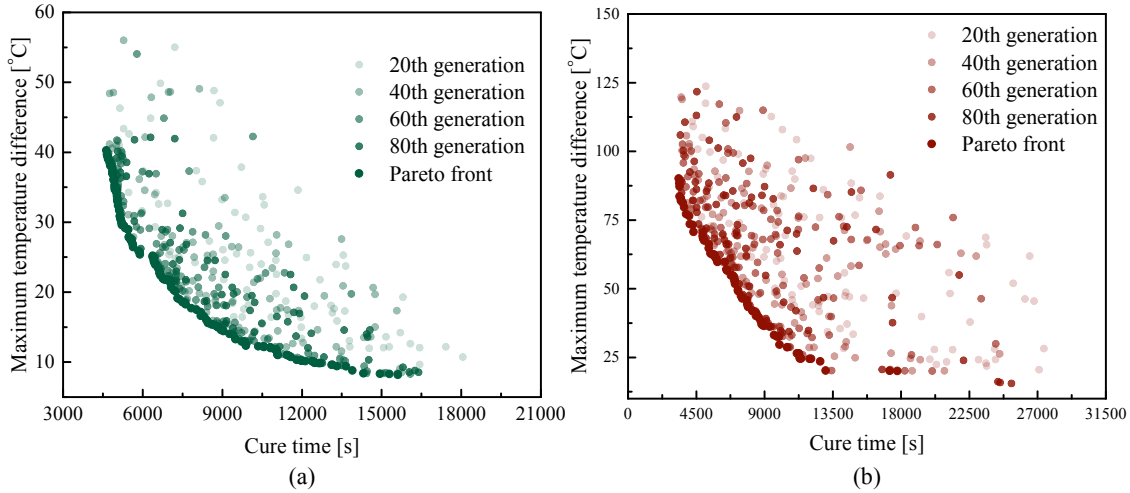

Figure 7: Pareto fronts for (a) thick and (b) ultra-thick laminates.

Fig 8. It can be seen that the result from original recommended profile presents long cure time and high temperature overshoot. For both the thick and ultra-thick laminates, the Pareto points of the two-dwell profile optimization are shifted up compared to the Pareto front of four-dwell profile optimization. With the same cure time, the four-dwell optimization result obtains a lower temperature overshoot. It is clearly shown that the increase of dwell expands the design space and generates the superior solutions. This improvement is more obvious for the ultra-thick laminate, as illustrated in Fig 8b. Compared with the two-dwell optimization, with the same cure time of 9000s, the maximum temperature overshoot by the four-dwell optimization is further reduced by 12 °C in the ultra-thick laminate and 6 °C in the thick laminate.

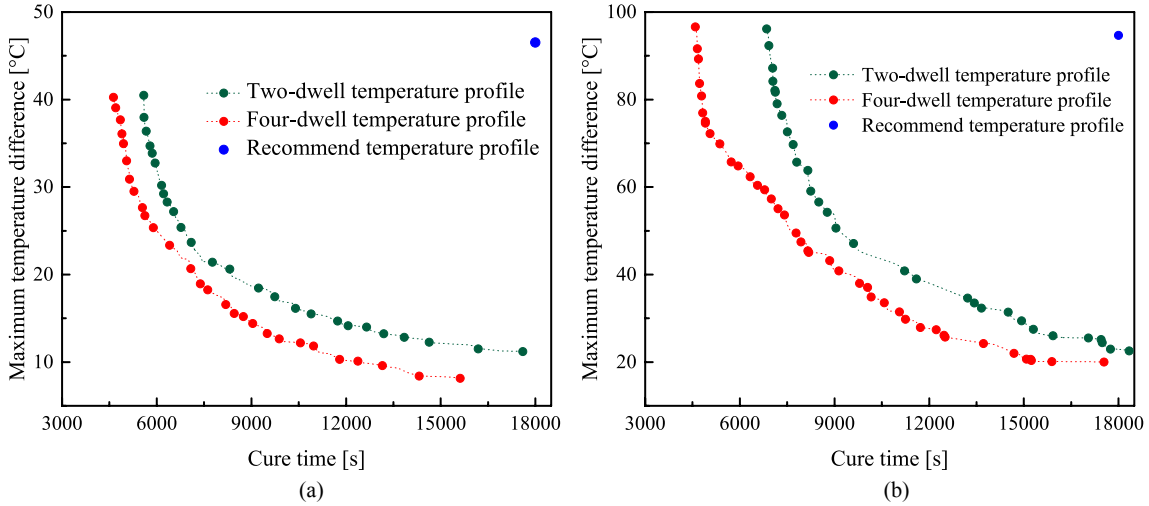

Figure 8: Optimization result for (a) thick and (b) ultra-thick laminates.

In the thick case, the evolution history of the temperature and degree of cure at center and bottom surface of laminate from the four-dwell optimization are shown in Fig 9a. The optimized value of design variables are listed in Table 6. The temperature of first and second dwell after optimization is much lower than the recommended profile. The decrease in temperature slows the cure reaction and avoids the dramatic accumulation of the reaction heat, which benefits the reduction of the temperature overshoot. After the second dwell, the center temperature starts to exceed the bottom surface temperature and the degree of cure is close to 0.5. Then the cure rate increases rapidly. At the end of the cure process, the degree of cure at the bottom surface is 0.92. The maximum difference of degree of cure is 0.11, which indicates that the distribution of degree

of cure is more uniform after optimization. The cure time and maximum temperature overshoot before and after optimization are shown in Table 7. Compared with the recommended profile, the four-dwell profile can reduce the cure time by 51.0% and temperature overshoot by 66.9%.

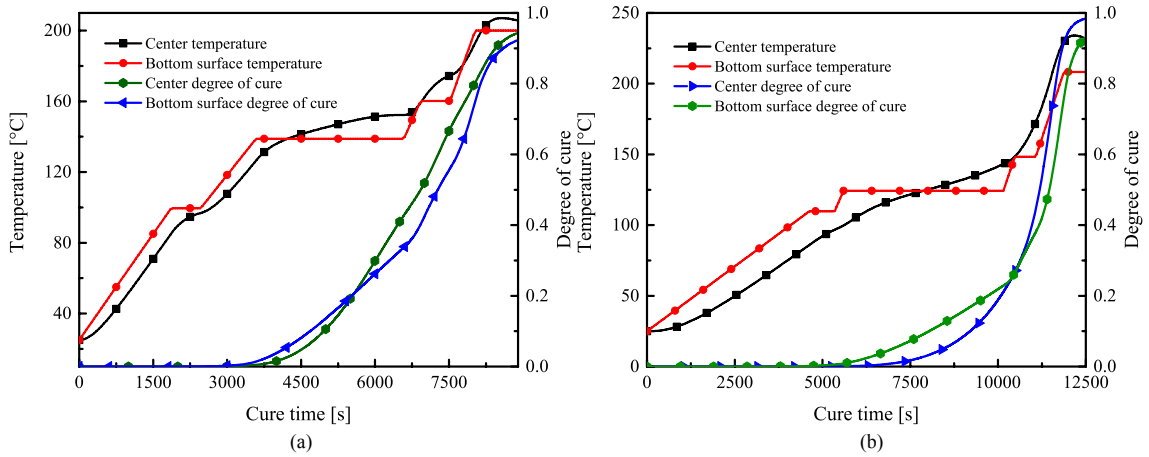

Figure 9: Evolution history of the temperature and degree of cure for (a) thick and (b) ultra-thick laminates

For the ultra-thick laminate, the evolution history of the temperature and degree of cure at center and bottom surface of laminate from the four-dwell optimization are shown in Fig 9b. Compared with the recommended profile, the first heating rate is significantly decreased. The first dwell temperature of the optimized profile is almost unchanged while the second dwell temperature is greatly reduced. The decreases in heating rate and the second dwell temperature is able to slow the cure reaction and thus avoids the dramatic accumulation of the reaction heat.

Moreover, the optimized profile increases the third and four heating rates and decreases the durations of the third and four dwells. By this way, the violent curing reaction could be translated from holding stage to heating stage. As a result, when the temperature and cure rate of the laminate center are increased due to exothermic heat generation and accumulation, the temperature and cure rate of the laminate surface are also increased by the heating air, which prevents the occurrence of large temperature difference between the center and the surface of laminate. Compared with the recommended profile, the four-dwell profile can reduce the cure time by 30.3% and temperature overshoot by 73.1%.

Pareto front can effectively demonstrate the relationship between the objective functions of the multi-objective optimization. Trade-off relationship is observed between the curing time and the

Table 6: Value of design variables in optimized profile.

	24mm laminate	50mm laminate
a_1, a_2, a_3, a_4 [°C/min]	2.3, 2.1, 3.6 , 4.8	1.1, 3.5, 4.5, 4.5
t_1, t_2, t_3, t_4 [s]	6000, 3000, 600, 840	720, 4560, 600, 600
ΔT_1 [°C]	64.6	85
ΔT_2, ΔT_3, ΔT_4 [°C]	39.1, 21.5, 39.8	14.4, 24.0, 60.0

Table 7: Simulation result of optimized and recommend profiles.

	Thick laminate		Ultra-thick laminate	
	Cure time[s]	Temperature difference[°C]	Cure time[s]	Temperature difference[°C]
Optimization	8837	15.37	12535	25.6
Recommend	18000	46.5	18000	94.6

maximum temperature difference from Fig 8. However, from the Pareto front results of Fig 8, only the relationship between the objective functions can be observed. It is difficult to understand the relationships between the design variables and the objective functions. Self-organizing map (SOM) can provide a visualized result and enlighten designer how the design variables affect the optimization objectives [35]. Therefore, in this study the relationships between the design variables and the objective functions for thick and ultra-thick laminates are visualized by using SOM.

Fig 10 presents the maps of the twelve design variables and two objectives of the four-dwell profile optimization of thick laminate. Each cluster in the map has a value and is represented by a specific color. The label of each map indicates the lower (blue color) and upper (yellow color) limits of the solutions of the design variable. The collection of the clusters in same location of each map constitutes an optimized cure profile. The corresponding objective values can be found in the same location of objective maps. Thus, the relationships between the design variables and the objective functions can be easily observed in a visualized way.

From Fig 10, it can be found that the color distribution of the maps of heating rates are similar with the map of maximum temperature difference, whereas opposite with the map of cure time. Therefore, in order to reduce the maximum temperature difference, the heating rates should be decreased, whereas to shorten the cure time, the heating rates should be increased. The influences of other variables can be derived by the same way. For instance, the maps of ΔT_i are opposite

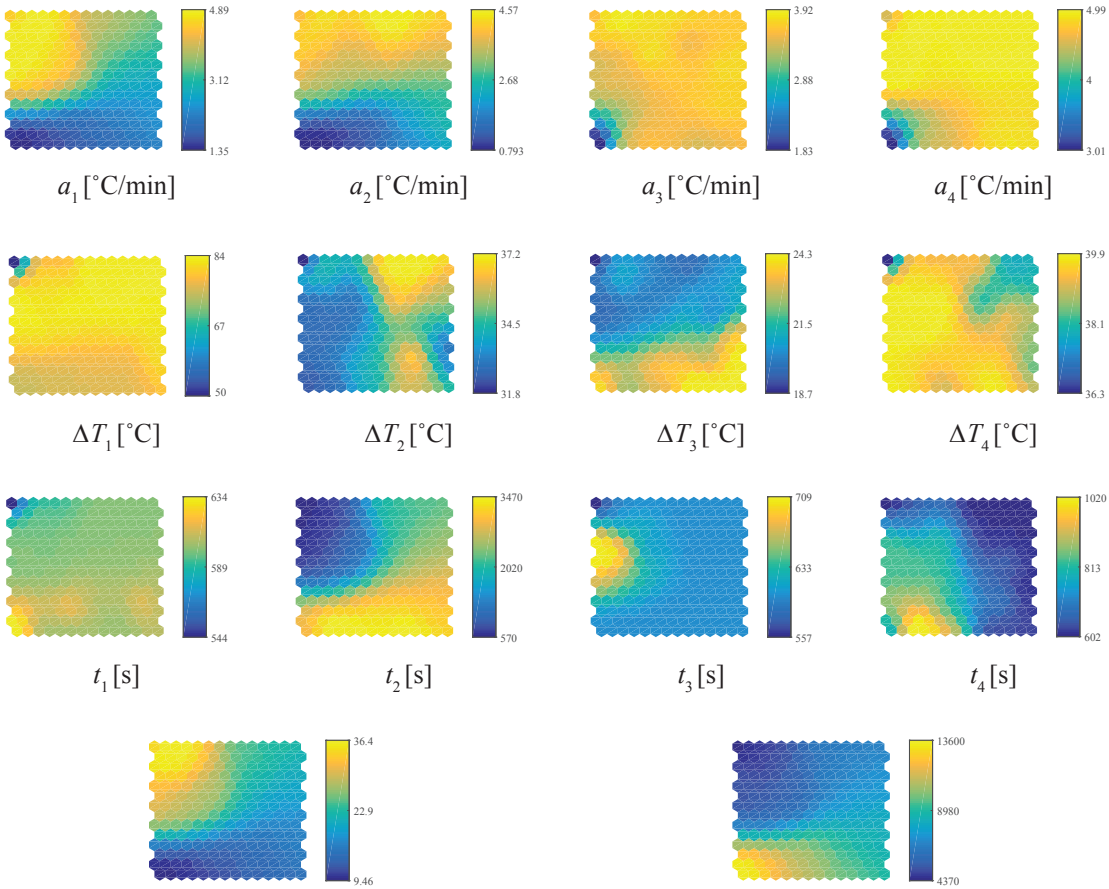

Figure 10: Self-organizing map of optimization result in thick laminate case.

with the map of maximum temperature difference and the maps of t_i are similar with the map of cure time. It can be concluded that the increase of the values of ΔT_i could reduce the maximum temperature difference. The cure time can be reduced by the decrease of t_i.

In the ultra-thick laminate, the relationships between the design variables and the objective functions are more complicated compared with the thick laminate. The maps of a_1 and ΔT_1 are similar with maximum temperature difference, whereas opposite with cure time. The maps of t_i have a similar color distribution with cure time. The maps of the other design variables indicate a complicated nonlinear relationship between the variables and the objective functions.

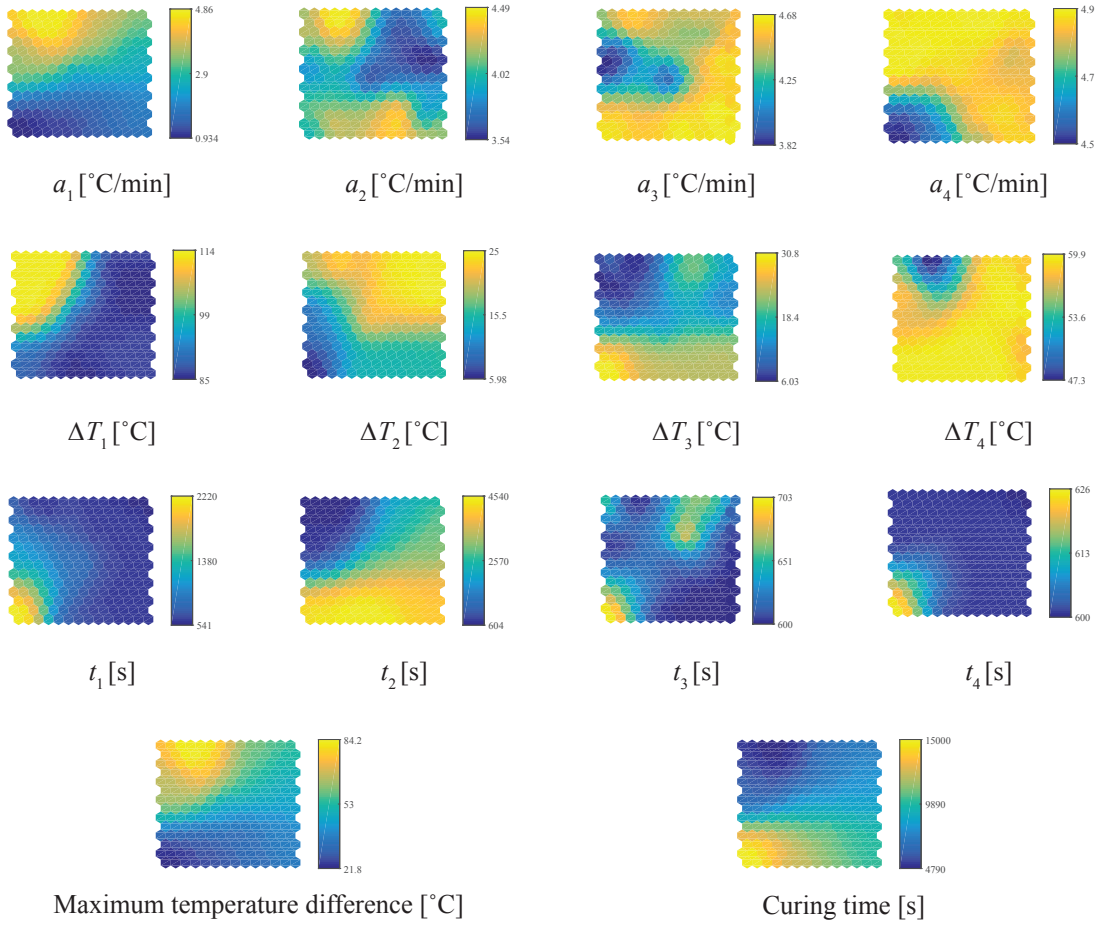

Figure 11: Self-organizing map of optimization result in ultra-thick laminate case.

5. Conclusions

A multi-objective optimization method is proposed to design the multi-dwell temperature profile of the CFRP composite laminates with large thickness. Based on the finite element analysis, thermo-chemical coupled cure simulation is performed to evaluate the evolutions of temperature and degree of cure of the composites. Through the optimization with NSGA-II algorithm, the maximum temperature difference and cure time are both significantly reduced. The two-dwell and four-dwell temperature profiles are both considered in the optimization to investigate the influence of the number of dwell on the optimization result. It is concluded that the four-dwell profile helps to achieve the optimization objective more effectively for the thick composite laminates. Compared with the recommended profile, the four-dwell profile can reduce the cure time by 51.0% (thick case) and 30.3% (ultra-thick case) and the maximum temperature difference by 66.9% (thick case) and 73.1% (ultra-thick case). Furthermore, the SOM is used to visualize the relationships between the design variables and the objectives. By the SOM analysis, it is possible to easily convey to the designer how the temperature profile variables affect the cure time and the temperature overshoot.

Acknowledgements

This work is supported by National Natural Science Foundation of China (11872310).

Author contribution

Wenchang Zhang: Conceptualization, Methodology, Writing - original draft, Conceptualization, Software, Data curation, Validation. Yingjie Xu: Investigation, Writing – review & editing, Funding acquisition, Supervision. Xinyu Hui: Methodology, Data curation, Validation. Weihong Zhang: Supervision, Visualization.

Availability of data and materials

The raw/processed data required to reproduce these findings cannot be shared publically but is available upon request.

Declarations

Ethical approval: Work was conducted ethically with no human test subjects.

Consent to participate: Work was conducted with no human test subjects.

Consent for publication: Work has consent to publish.

Competing interests: The authors declare that they have no competing interests.

References

[1] A. Kootsookos, A. Mouritz, Seawater durability of glass- and carbon-polymer composites, Composites Science and Technology 64 (10) (2004) 1503–1511. doi:https://doi.org/10.1016/j.compscitech.2003.10.019.

[2] W.-B. Young, Compacting pressure and cure cycle for processing of thick composite laminates, Composites Science and Technology 54 (3) (1995) 299–306. doi:https://doi.org/10.1016/0266-3538(95)00067-4.

[3] G. Struzziero, J. Teuwen, A. Skordos, Numerical optimisation of thermoset composites manufacturing processes: A review, Composites Part A: Applied Science and Manufacturing 124 (2019) 105499. doi:https://doi.org/10.1016/j.compositesa.2019.105499.

[4] X. Hui, Y. Xu, W. Zhang, An integrated modeling of the curing process and transverse tensile damage of unidirectional cfrp composites, Composite Structures 263 (2021) 113681. doi:https://doi.org/10.1016/j.compstruct.2021.113681.

[5] C. Li, M. Cao, R. Wang, Z. Wang, Y. Qiao, L. Wan, Q. Tian, H. Liu, D. Zhang, T. Liang, C. Tang, Fiber-optic composite cure sensor: monitoring the curing process of composite material based on intensity modulation, Composites Science and Technology 63 (12) (2003) 1749–1758. doi:https://doi.org/10.1016/S0266-3538(03)00118-0.

[6] R. L. Levy, S. D. Schwab, Monitoring the composite curing process with a fluorescence-based fiber-optic sensor, Polymer Composites 12 (2) (1991) 96–101. doi:https://doi.org/10.1002/pc.750120205.

[7] P. Hubert, Aspects of flow and compaction of laminated composite shapes during cure, Ph.D. thesis, University of British Columbia (1996).

[8] C. Griffis, R. Masumura, C. Chang, Thermal response of graphite epoxy composite subjected to rapid heating, Journal of Composite Materials 15 (5) (1981) 427–442. doi:https://doi.org/10.1177/002199838101500503.

[9] H. C. Park, N. S. Goo, K. J. Min, K. J. Yoon, Three-dimensional cure simulation of composite structures by the finite element method, Composite Structures 62 (1) (2003) 51–57. doi:https://doi.org/10.1016/S0263-8223(03)00083-7.

[10] T. Twardowski, S. Lin, P. Geil, Curing in thick composite laminates: Experiment and simulation, Journal of Composite Materials 27 (3) (1993) 216–250. doi:https://doi.org/10.1177/002199839302700301.

[11] S. Y. Pusatcioglu, J. C. Hassler, A. L. Fricke, H. A. McGee Jr., Effect of temperature gradients on cure and stress gradients in thick thermoset castings, Journal of Applied Polymer Science 25 (3) (1980) 381–393. doi:https://doi.org/10.1002/app.1980.070250305.

[12] S. Yi, H. H. Hilton, Effects of thermo-mechanical properties of composites on viscosity, temperature and degree of cure in thick thermosetting composite laminates during curing process, Journal of Composite Materials 32 (7) (1998) 600–622. doi:https://doi.org/10.1177/002199839803200701.

[13] J. H. Oh, D. G. Lee, Cure cycle for thick glass/epoxy composite laminates, Journal of Composite Materials 36 (1) (2002) 19–45. doi:https://doi.org/10.1177/0021998302036001300.

[14] M. Li, C. L. Tucker III, Optimal curing for thermoset matrix composites: Thermochemical and consolidation considerations, Polymer Composites 23 (5) (2002) 739–757. doi:https://doi.org/10.1002/pc.10473.

[15] E. Ruiz, F. Trochu, Multi-criteria thermal optimization in liquid composite molding to reduce processing stresses and cycle time, Composites Part A: Applied Science and Manufacturing 37 (6) (2006) 913–924. doi:https://doi.org/10.1016/j.compositesa.2005.06.010.

[16] G. J. Kennedy, J. S. Hansen, The hybrid-adjoint method: a semi-analytic gradient evaluation technique applied to composite cure cycle optimization, Optimization and Engineering 11 (1) (2010) 23–43. doi:https://doi.org/10.1007/s11081-008-9068-9.

[17] M. Vafayan, M. H. R. Ghoreishy, H. Abedini, M. H. Beheshty, Development of an optimized thermal cure cycle for a complex-shape composite part using a coupled finite element/genetic algorithm technique, Iranian Polymer Journal 24 (6) (2015) 459–469. doi:https://doi.org/10.1007/s13726-015-0337-0.

[18] H. Wang, L. Chen, F. Ye, J. Wang, A multi-hierarchical successive optimization method for reduction of spring-back in autoclave forming, Composite Structures 188 (2018) 143–158. doi:https://doi.org/10.1016/j.compstruct.2018.01.010.

[19] D. Aleksendrić, C. Bellini, P. Carlone, V. Ćirović, F. Rubino, L. Sorrentino, Neural-fuzzy optimization of thick composites curing process, Materials and Manufacturing Processes 34 (3) (2019) 262–273. doi:https://doi.org/10.1080/10426914.2018.1512116.

[20] G. Struzziero, A. Skordos, Multi-objective optimisation of the cure of thick components, Composites Part A: Applied Science and Manufacturing 93 (2017) 126–136. doi:https://doi.org/10.1016/j.compositesa.2016.11.014.

[21] P. Shah, V. Halls, J. Zheng, R. Batra, Optimal cure cycle parameters for minimizing residual stresses in fiber-reinforced polymer composite laminates, Journal of Composite Materials 52 (6) (2018) 773–792. doi:https://doi.org/10.1177/0021998317714317.

[22] D. Dolkun, W. Zhu, Q. Xu, Y. Ke, Optimization of cure profile for thick composite parts based on finite element

analysis and genetic algorithm, Journal of Composite Materials 52 (28) (2018) 3885–3894. doi:https://doi.org/10.1177/0021998318771458.

[23] L. Sorrentino, L. Tersigni, A method for cure process design of thick composite components manufactured by closed die technology, Applied Composite Materials 19 (1) (2012) 31–45. doi:https://doi.org/10.1007/s10443-010-9179-2.

[24] L. Sorrentino, C. Bellini, Validation of a methodology for cure process optimization of thick composite laminates, Polymer-Plastics Technology and Engineering 54 (17) (2015) 1803–1811. doi:https://doi.org/10.1080/03602559.2015.1050513.

[25] P. E. Jahromi, A. Shojaei, S. M. Reza Pishvaie, Prediction and optimization of cure cycle of thick fiber-reinforced composite parts using dynamic artificial neural networks, Journal of reinforced plastics and composites 31 (18) (2012) 1201–1215. doi:https://doi.org/10.1177/0731684412451937.

[26] M. Hojjati, S. Hoa, Curing simulation of thick thermosetting composites, Composites Manufacturing 5 (3) (1994) 159–169. doi:https://doi.org/10.1016/0956-7143(94)90025-6.

[27] K. Cole, J. Hechler, D. Noel, A new approach to modeling the cure kinetics of epoxy/amine thermosetting resins. 2. application to a typical system based on bis [4-(diglycidylamino) phenyl] methane and bis (4-aminophenyl) sulfone, Macromolecules 24 (11) (1991) 3098–3110.

[28] A. A. Johnston, An integrated model of the development of process-induced deformation in autoclave processing of composite structures, Ph.D. thesis, University of British Columbia (1997).

[29] G. F. Abdelal, A. Robotham, W. Cantwell, Autoclave cure simulation of composite structures applying implicit and explicit fe techniques, International Journal of Mechanics and Materials in Design 9 (1) (2013) 55–63. doi:https://doi.org/10.1007/s10999-012-9205-7.

[30] X. Li, J. Wang, S. Li, A. Ding, Cure-induced temperature gradient in laminated composite plate: Numerical simulation and experimental measurement, Composite Structures 253 (2020) 112822. doi:https://doi.org/10.1016/j.compstruct.2020.112822.

[31] V. Antonucci, M. Giordano, S. Inserraimparato, L. Nicolais, Analysis of heat transfer in autoclave technology, Polymer composites 22 (5) (2001) 613–620. doi:https://doi.org/10.1002/pc.10564.

[32] L. Esposito, L. Sorrentino, F. Penta, C. Bellini, Effect of curing overheating on interlaminar shear strength and its modelling in thick frp laminates, The International Journal of Advanced Manufacturing Technology 87 (5) (2016) 2213–2220. doi:https://doi.org/10.1007/s00170-016-8613-5.

[33] E. Fallah-Mehdipour, O. Bozorg Haddad, M. M. Rezapour Tabari, M. A. Mariño, Extraction of decision alternatives in construction management projects: Application and adaptation of nsga-ii and mopso, Expert Systems with Applications 39 (3) (2012) 2794–2803. doi:https://doi.org/10.1016/j.eswa.2011.08.139.

[34] K. Deb, A. Pratap, S. Agarwal, T. Meyarivan, A fast and elitist multiobjective genetic algorithm: Nsga-ii, IEEE Transactions on Evolutionary Computation 6 (2) (2002) 182–197. doi:https://doi.org/10.1109/4235.

996017.

[35] R. Matsuzaki, R. Yokoyama, T. Kobara, T. Tachikawa, Multi-objective curing optimization of carbon fiber composite materials using data assimilation and localized heating, Composites Part A: Applied Science and Manufacturing 119 (2019) 61–72. doi:https://doi.org/10.1016/j.compositesa.2019.01.021.

Figures

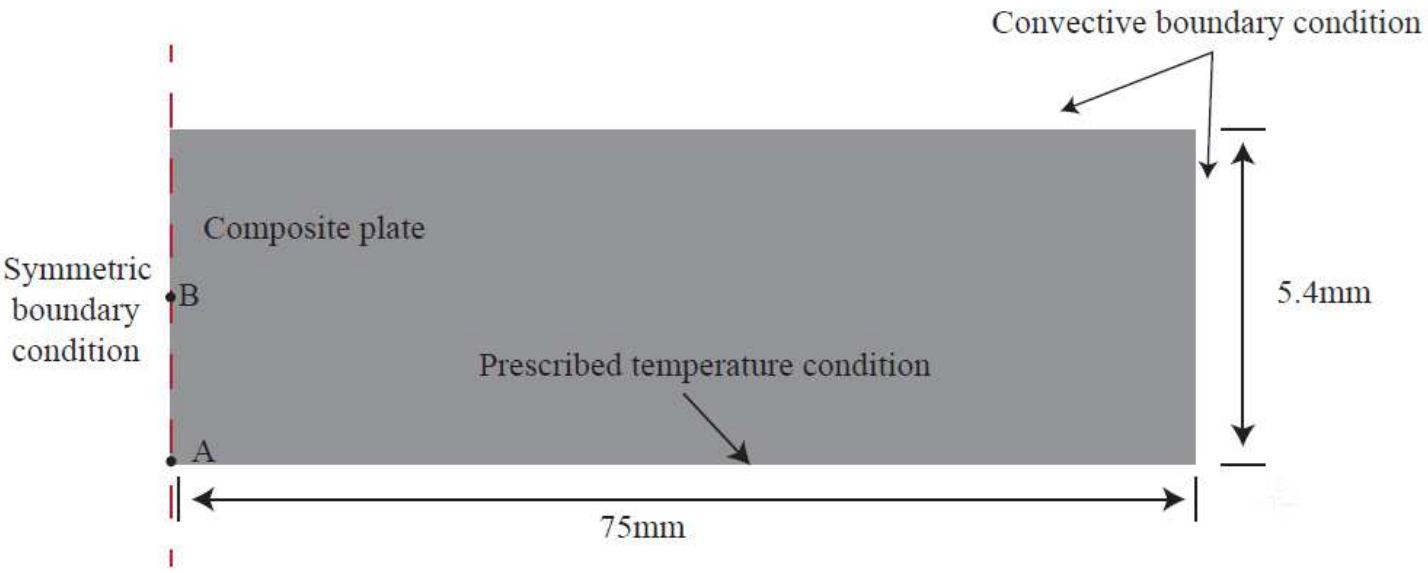

Figure 1

Schematic of the validated model.

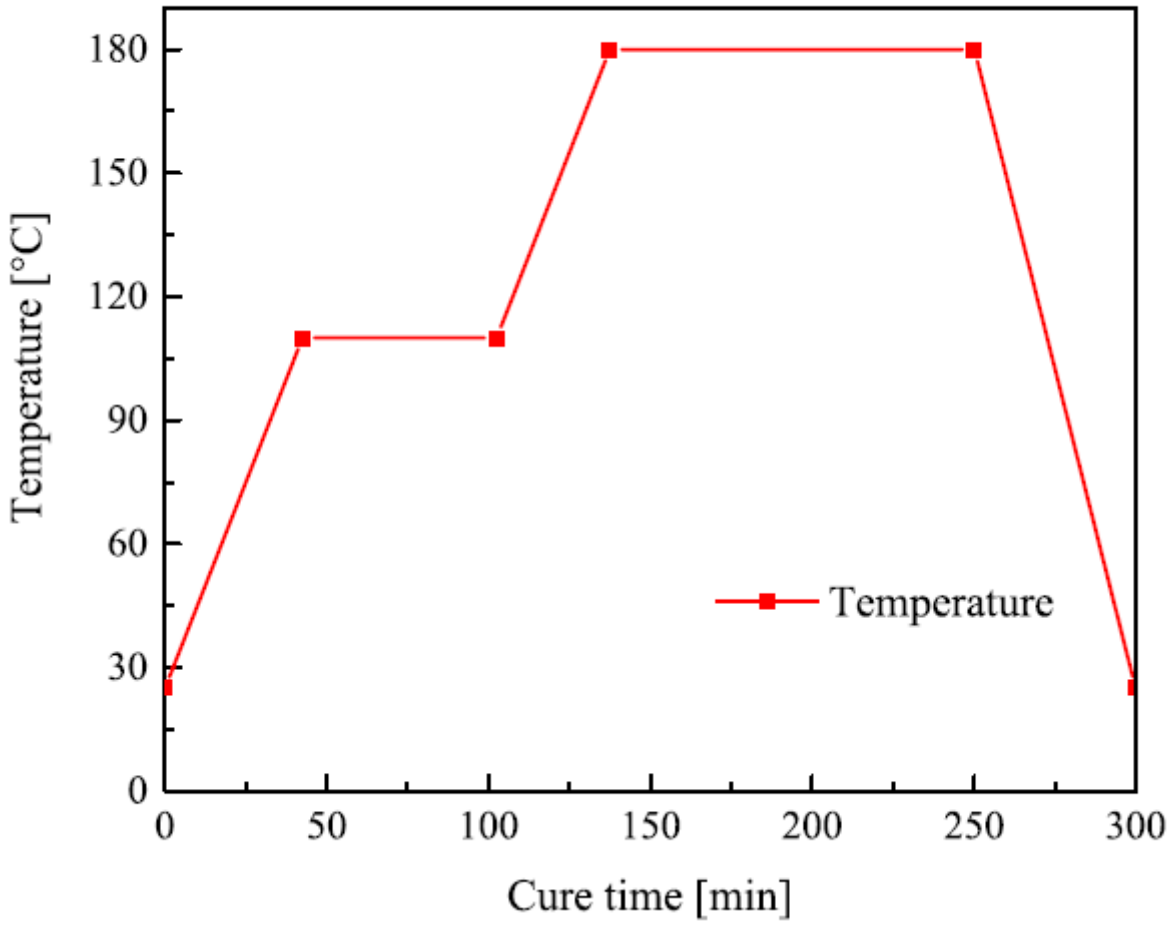

Figure 2

Curing temperature profile used for model validation.

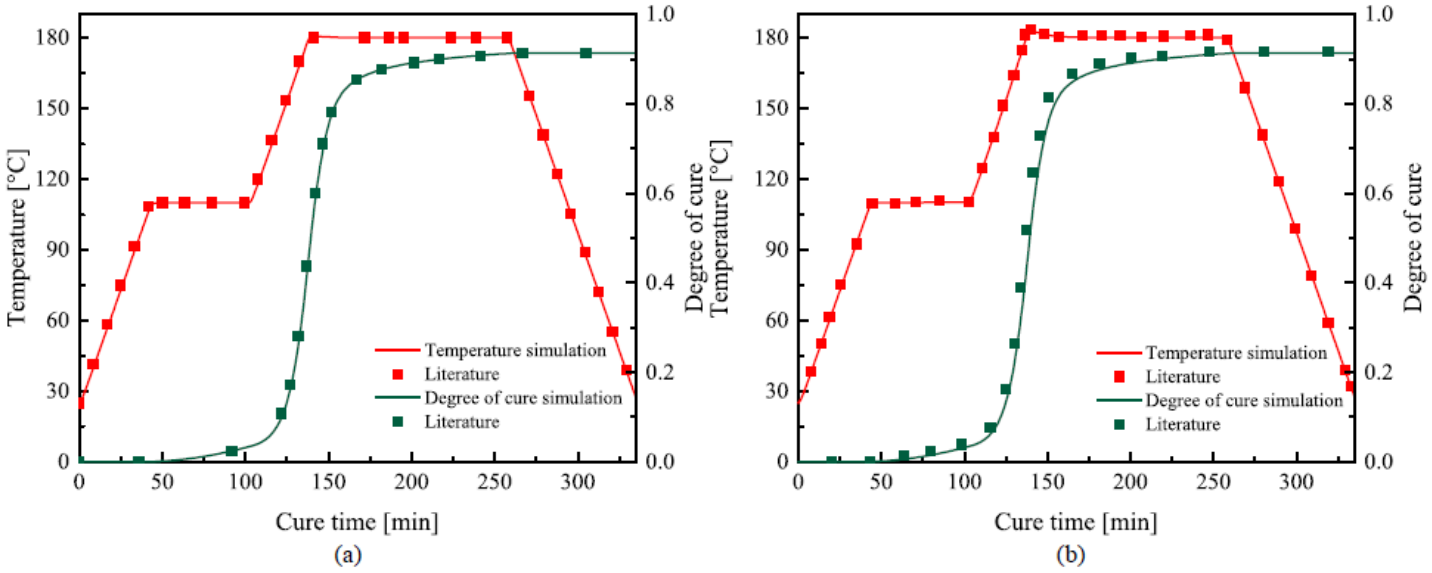

Figure 3

Comparison of simulation result and literature data: (a) Point A, (b) Point B.

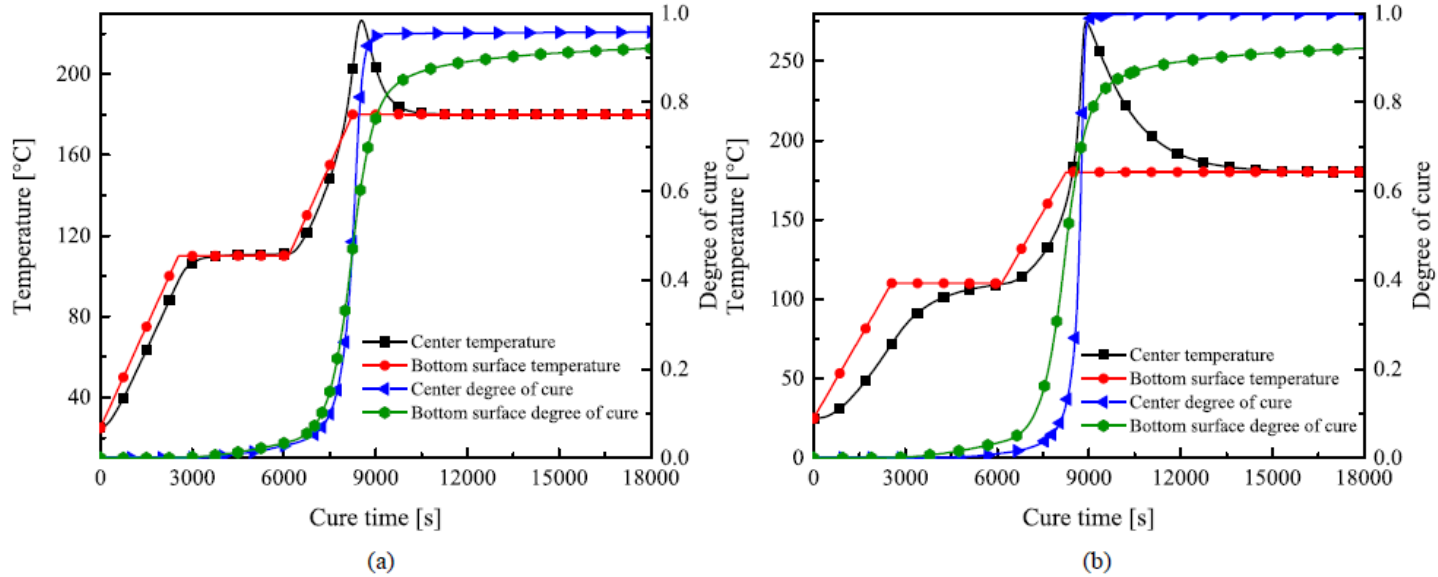

Figure 4

Simulation result of recommended cure profile for (a) thick laminate and (b) ultra-thick laminate.

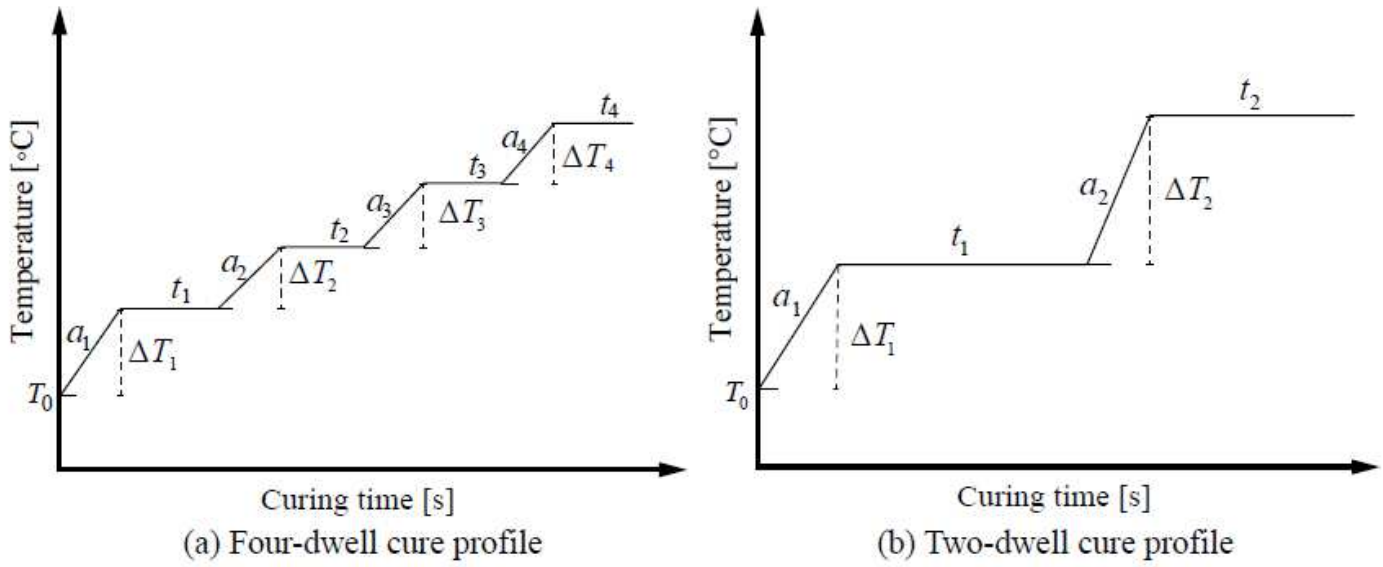

Figure 5

Temperature profiles to be optimized: (a) Four-dwell profile, (b) Two-dwell profile.

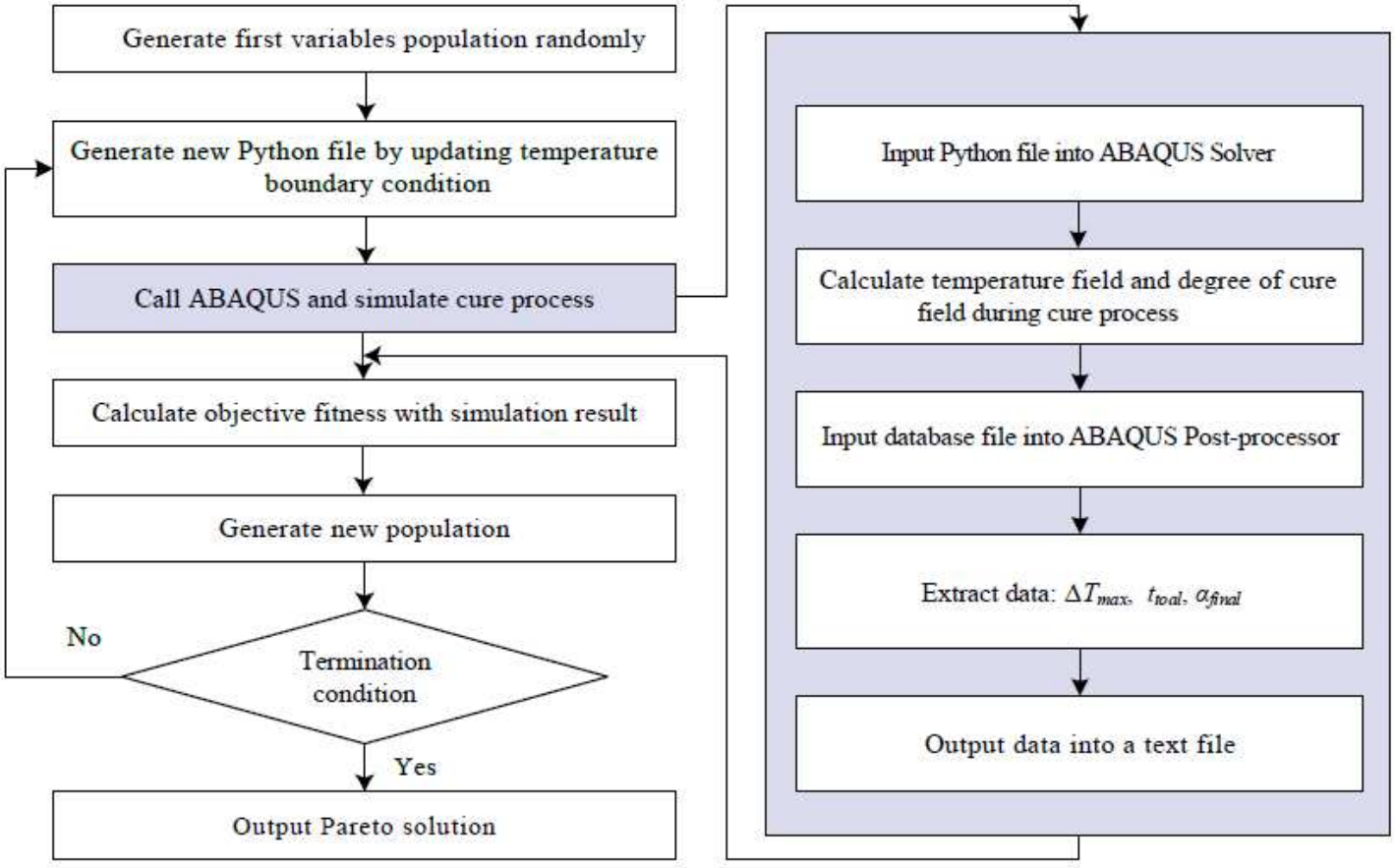

Figure 6

The flowchart of optimization.

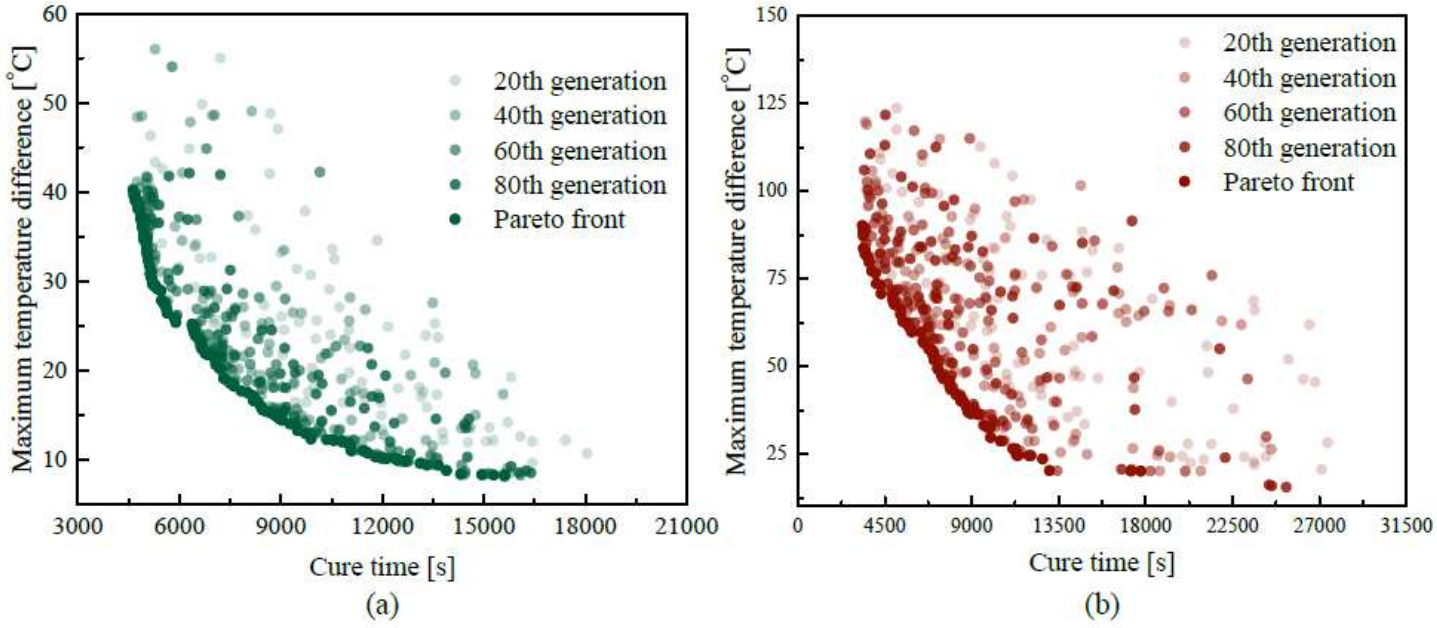

Figure 7

Pareto fronts for (a) thick and (b) ultra-thick laminates.

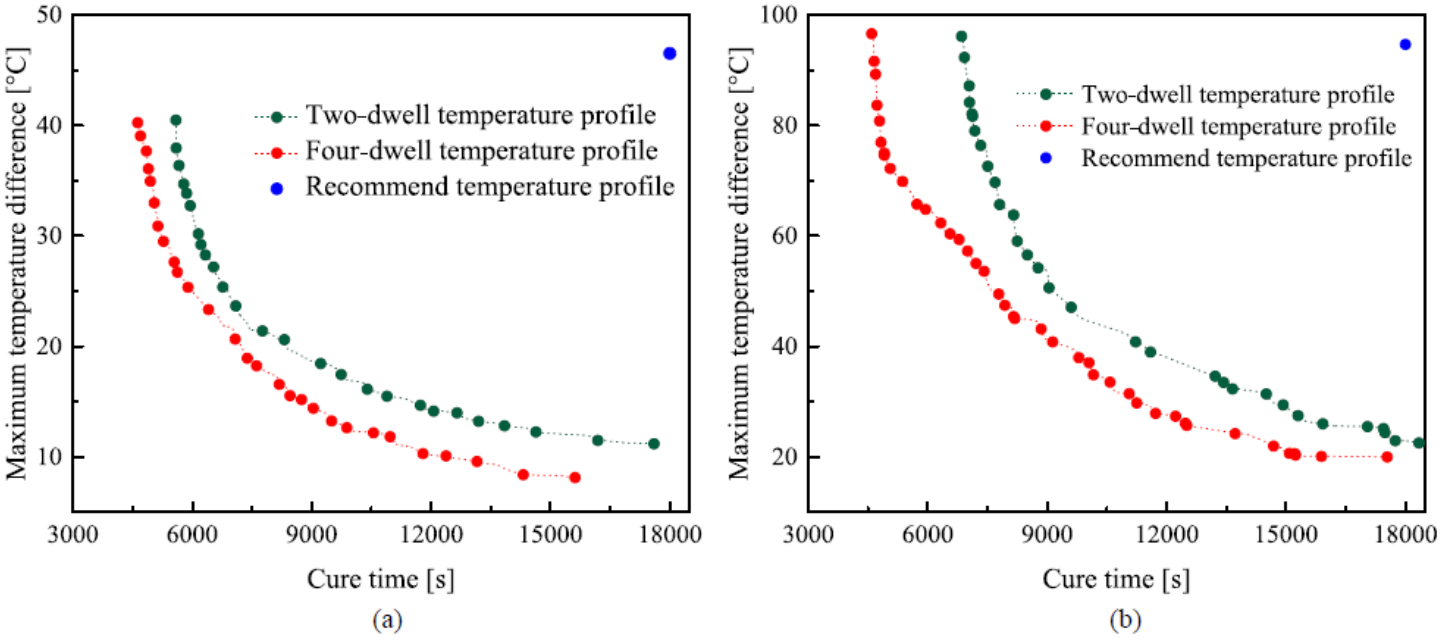

Figure 8

Optimization result for (a) thick and (b) ultra-thick laminates.

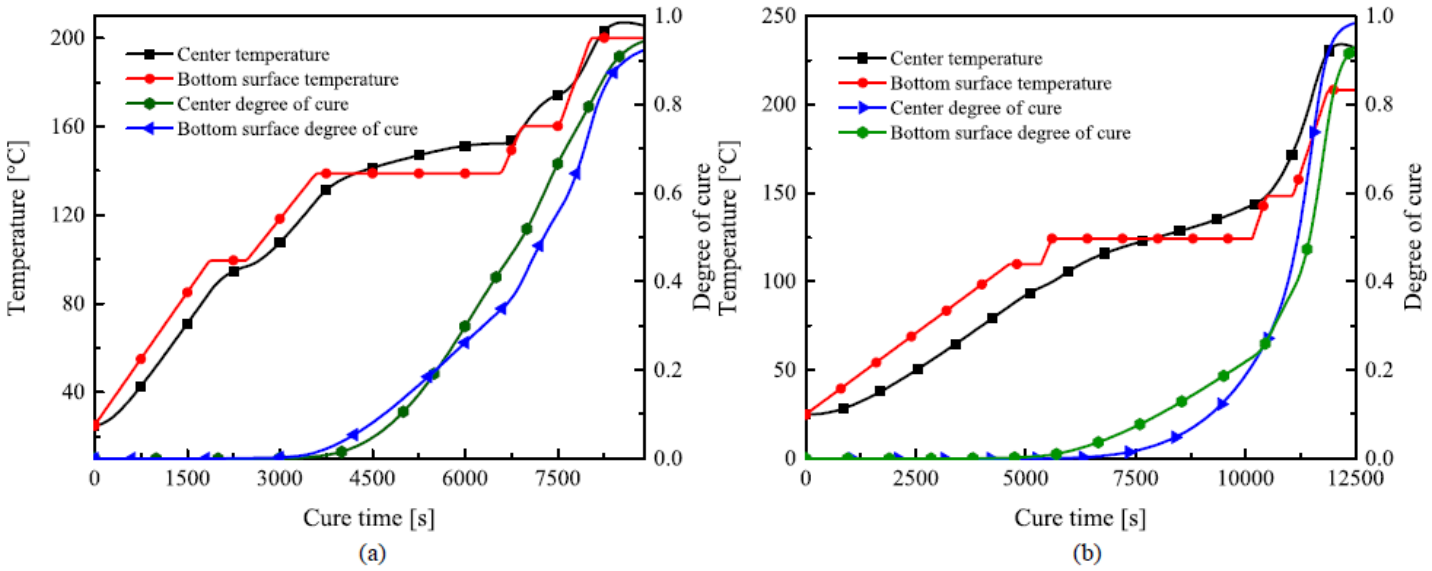

Figure 9

Evolution history of the temperature and degree of cure for (a) thick and (b) ultra-thick laminates

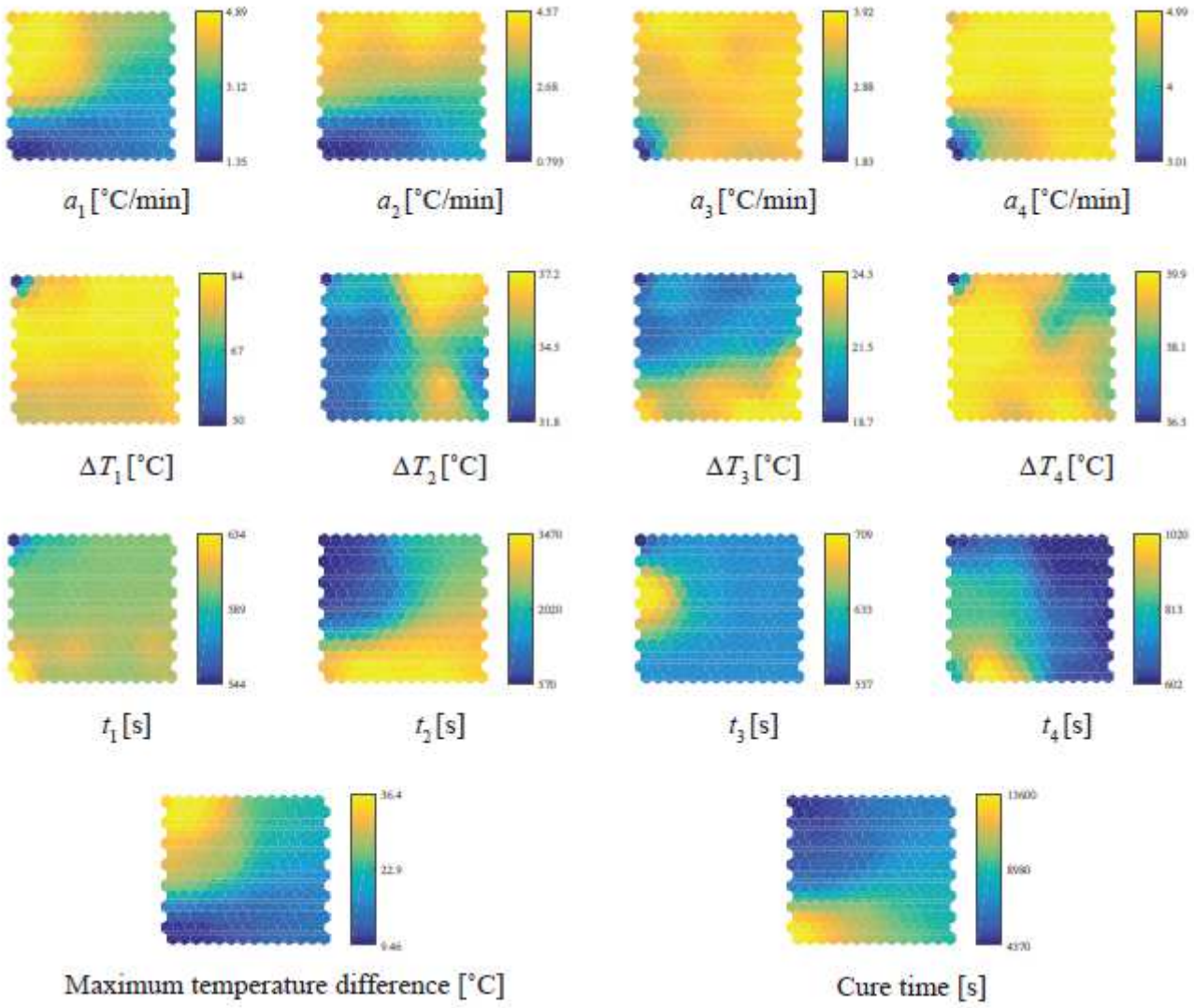

Figure 10

Self-organizing map of optimization result in thick laminate case.

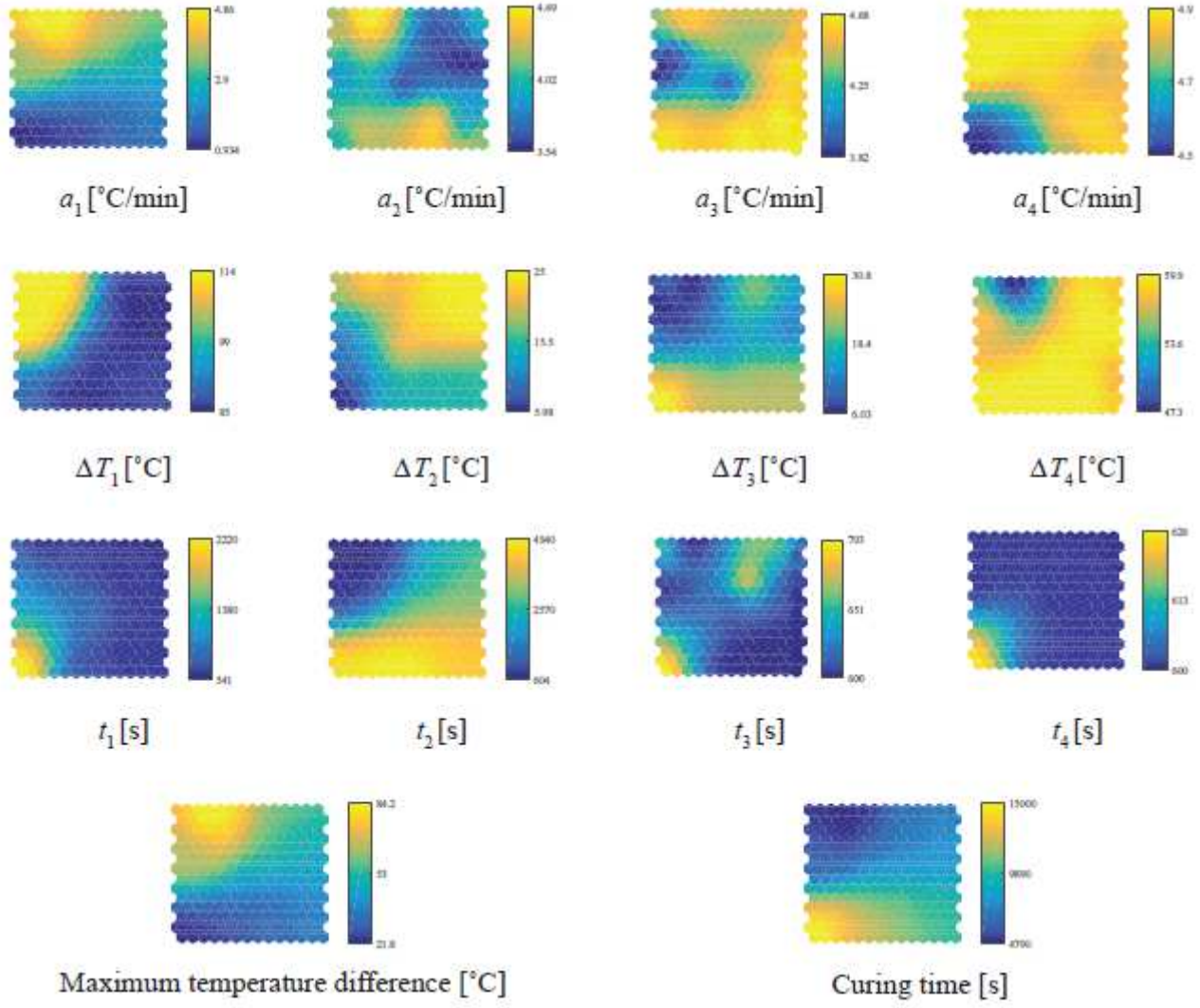

Figure 11

Self-organizing map of optimization result in ultra-thick laminate case.